

Empirical description of transverse momentum spectra of identified particles produced in proton-proton collisions at $\sqrt{s} = 200$ GeV

Pei-Pin Yang^{1,2}, Fu-Hu Liu^{1,*}, and Raghunath Sahoo^{3,†}

¹*Institute of Theoretical Physics and State Key Laboratory of Quantum Optics and Quantum Optics Devices, Shanxi University, Taiyuan, Shanxi 030006, China*

²*Bogoliubov Laboratory for Theoretical Physics, Joint Institute for Nuclear Research, 141980 Dubna, Russia and*

³*Discipline of Physics, School of Basic Sciences, Indian Institute of Technology Indore, Simrol, Indore 453552, India*

Abstract: Transverse momentum spectra of identified particles produced in high energy proton-proton ($p + p$) collisions are empirically described in the framework of participant quark model or the multisource model at the quark level, in which the source itself is exactly the participant quark. Each participant (constituent) quark contributes to the transverse momentum spectrum, which are described by a revised Tsallis-Pareto-type (TP-like) function. The transverse momentum spectrum of the hadron is the fold of two or more TP-like functions. For a lepton, the transverse momentum spectrum is the fold of two TP-like functions due to two participant quarks, e.g. projectile and target quarks, taking part in the collisions. A discussed theoretical approach seems to describe the $p+p$ collisions data at center-of-mass energy $\sqrt{s} = 200$ GeV very well.

Keywords: Transverse momentum spectra, identified particles, empirical description, TP-like function

PACS: 12.40.Ee, 13.85.Hd, 24.10.Pa

I. INTRODUCTION

As one of the “first day” measurable quantities, the transverse momentum (p_T) spectra of various particles produced in high energy proton-proton (hadron-hadron), proton-nucleus (hadron-nucleus), and nucleus-nucleus collisions are of special importance because, it reveals about the temperature and collectivity in the produced systems. The distribution range of p_T is generally very wide, from 0 to more than 100 GeV/c, which is collision energy dependent. In very low-, low-, high-, and very high- p_T regions [1], the shapes of p_T spectrum for given particles are possibly different from each other. In some cases, the differences are very large and the spectra show different empirical laws.

Generally, the spectrum in (very) low- p_T region is contributed by (resonance decays or other) soft excitation process. The spectrum in (very) high- p_T region is naturally contributed by (very) hard scattering process. There is no such boundary in p_T to separate soft and

hard processes. At a given collision energy, for different collision species, looking into the spectral shape, a theoretical function that best fits to the p_T -spectra is usually chosen to extract information like rapidity density, dN/dy , kinetic freeze-out temperature, T_{kin} or T_0 and average radial flow velocity, $\langle \beta_T \rangle$ or β_T . The low- p_T region up to $\sim 2\text{--}3$ GeV/c is well described by a Boltzmann-Gibbs function, whereas the high- p_T part is dominated by a power-law tail. It is interesting to note that there are many different functions, sometimes motivated by experimental trend of the data or sometimes theoretically, to have a proper spectral description thereby leading to a physical picture. The widely used functions are:

1. An exponential function in p_T or m_T [2]:

$$f(p_T) = p_T \times A \times \left(e^{-p_T/T} \right) \times \frac{e^{m_0/T}}{T^2 + Tm_0}, \quad (1)$$

$$f(p_T) = p_T \times A \times \left(e^{-m_T/T} \right) \times \frac{e^{m_0/T}}{T^2 + Tm_0}. \quad (2)$$

Here, A is the normalization constant, T is the effective temperature (thermal temperature and

*E-mail: fuhuli@163.com; fuhuli@sxu.edu.cn

†E-mail: raghunath.phy@gmail.com; Raghunath.Sahoo@cern.ch

collective radial flow) and $m_T = \sqrt{p_T^2 + m_0^2}$ is the transverse mass, with m_0 being the identified particle rest mass.

2. A Boltzmann distribution:

$$f(p_T) = p_T \times A \times m_T \times \left(e^{-m_T/T} \right) \times \frac{e^{m_0/T}}{2T^3 + 2T^2 m_0 + T m_0^2}. \quad (3)$$

3. Bose–Einstein/Fermi–Dirac distribution:

$$f(p_T) = p_T \times A \times m_T \times \frac{1}{e^{m_T/T} \mp 1} \times \left(e^{m_0/T} \mp 1 \right), \quad (4)$$

4. Power-law or Hagedorn function [3]:

$$f(p_T) = p_T \times A \times \left(1 + \frac{p_T}{p_0} \right)^{-n} \rightarrow \begin{cases} \exp\left(-\frac{np_T}{p_0}\right), & \text{for } p_T \rightarrow 0, \\ \left(\frac{p_0}{p_T}\right)^n, & \text{for } p_T \rightarrow \infty, \end{cases} \quad (5)$$

where p_0 and n are fitting parameters. This becomes a purely exponential function for small p_T and a purely power-law function for large p_T values.

5. Tsallis–Lévy [4, 5] or Tsallis–Pareto-type function [4, 6]:

$$f(p_T) = p_T \times \frac{A(n-1)(n-2)}{nT[nT + m_0(n-2)]} \times \left(1 + \frac{m_T - m_0}{nT} \right)^{-n}. \quad (6)$$

Note here that a multiplicative pre-factor of p_T in the above functions are used assuming that the p_T -spectra do not have a p_T factor in the denominator (see the expression for the invariant yield) and all the functions are normalized so that the integral of the functions provides the value of “ A ”. When the first three functions describe the p_T -spectra up to a low p_T around 2–3 GeV/c, the fourth function i.e. the power-law describes the high- p_T part of the spectrum. The last two functions (power-law or Hagedorn function and Tsallis–Lévy or Tsallis–Pareto-type function), which are more empirical in nature, lack with a microscopic picture, however, describe the full spectra. The Tsallis distribution function, while

describing the spectra in $p+p$ collisions, has brought up the concept of non-extensive entropy, contrary to the low- p_T domain pointing to an equilibrated system usually described by Boltzmann–Gibbs extensive entropy.

The two behaviors in (very) low- and (very) high- p_T regions are difficult to coordinate simultaneously by a simple probability density function. Instead, one can use a two-component function [7], the first component $f_1(p_T)$ is for the (very) low- p_T region and the second component $f_2(p_T)$ is for the (very) high- p_T region, to superpose a new function $f(p_T)$ to fit the p_T spectra. There are two forms of superpositions, $f(p_T) = kf_1(p_T) + (1-k)f_2(p_T)$ or $f(p_T) = A_1\theta(p_1 - p_T)f_1(p_T) + A_2\theta(p_T - p_1)f_2(p_T)$ [3, 8, 9], where k denotes the contribution fraction of the first component, A_1 and A_2 are constants which make the two components are equal to each other at $p_T = p_1$, and $\theta(x)$ is the usual step function which satisfies $\theta(x) = 0$ if $x < 0$ and $\theta(x) = 1$ if $x \geq 0$.

It is known that there are entanglements in determining parameters in the two components in the first superposition [8]. There is possibly a non-smooth interlinkage at $p_T = p_1$ between the two components in the second superposition [9]. These two issues are not our expectation. To avoid the entanglements and non-smooth interlinkage, we hope to use a new function to fit simultaneously the spectra in whole p_T region for various particles. After sounding many functions out, a Tsallis–Pareto-type function [4, 6] which empirically describes both the low- p_T exponential and the high- p_T power-law [10–13] is the closest to our target, though the Tsallis–Pareto-type function is needed to revise in some cases.

In this work, to describe the spectra in whole p_T range which includes (very) low and (very) high p_T regions, the Tsallis–Pareto-type function is empirically revised by a simple method. To describe the spectra in whole p_T range as accurately as possible, the contribution of participant quark to the spectrum is also empirically taken to be the revised Tsallis–Pareto-type (TP-like) function with another set of parameters. Then, the p_T distribution of given particles is the fold of a few TP-like functions. To describe the spectra of identified particles in whole p_T range, both the TP-like function and the fold of a few TP-like functions are used to fit the data measured in proton-proton ($p+p$) collisions at center-of-mass energy $\sqrt{s} = 200$ GeV by the PHENIX Collaboration [14–18].

The remainder of this paper is structured as follows. The formalism and method are described in Section 2. Results and discussion are given in Section 3. In Section 4, we summarize our main observations and conclusions.

II. FORMALISM AND METHOD

According to refs. [4, 6], the Tsallis–Pareto-type function which empirically describes both the low- p_T exponential and the high- p_T power-law can be simplified presented as [10–13],

$$f(p_T) = C \times p_T \times \left(1 + \frac{\sqrt{p_T^2 + m_0^2} - m_0}{nT} \right)^{-n} \quad (7)$$

in terms of p_T probability density function, where the parameter T describes the excitation degree of the considered source, the parameter n describes the degree of non-equilibrium of the considered source, and C is the normalization constant which depends on T , n , and m_0 . Equation (7) is in fact a rewrite of Eq. (6).

As an empirical formula, the Tsallis–Pareto-type function is successful in the description of p_T spectra in many cases. However, our exploratory analysis shows that Eq. (7) is not accurate in describing the spectra in whole p_T range in some cases. In particular, Eq. (7) cannot describe flexibility the spectra in very low- p_T region, which is contributed by the resonance decays. We would like to revise empirically Eq. (7) by adding a power index a_0 on p_T . After the revision, we have

$$f(p_T) = C \times p_T^{a_0} \times \left(1 + \frac{\sqrt{p_T^2 + m_0^2} - m_0}{nT} \right)^{-n}, \quad (8)$$

where C is the normalization constant which is different from that in Eq. (7). To be convenient, the two normalization constants in Eqs. (7) and (8) are denoted by the same symbol C . Eq. (8) can be used to fit the spectra in whole p_T range. The revised Tsallis–Pareto-type function [Eq. (8)] is called the TP-like function by us.

Our exploratory analysis shows that Eq. (8) is not accurate in describing the spectra in whole p_T range, too, though it is more accurate than Eq. (7). To obtain accurate results, the contribution (p_{ti}) of the i -th

participant quark to p_T is assumed to obey

$$f_i(p_{ti}) = C_i \times p_{ti}^{a_0} \times \left(1 + \frac{\sqrt{p_{ti}^2 + m_{0i}^2} - m_{0i}}{nT} \right)^{-n}, \quad (9)$$

where the subscript i is used for the quantities related to the participant quark i , and m_{0i} is empirically the constituent mass of the considered quark i . The value of i can be 2 or 3 even 4 or 5 due to the number of participant (or constituent) quarks. Eq. (9) is also the TP-like function with different mass from Eq. (8).

It should be noted that m_0 in Eq. (8) is for a particle, and m_{0i} in Eq. (9) is for the quark i . For example, if we study the p_T spectrum of protons, we have $m_0 = 0.938$ GeV/c^2 and $m_{01} = m_{02} = m_{03} = 0.31$ GeV/c^2 . In the case of studying the p_T spectrum of photons, we have $m_0 = 0$ and $m_{01} = m_{02} = 0.31$ GeV/c^2 if we assume that two lightest quarks taking part in the collision on photon production.

There are two participant quarks to constitute usually mesons, namely the quarks 1 and 2. The p_T spectra of mesons are the fold of two TP-like functions. We have

$$\begin{aligned} f(p_T) &= \int_0^{p_T} f_1(p_{t1}) f_2(p_T - p_{t1}) dp_{t1} \\ &= \int_0^{p_T} f_2(p_{t2}) f_1(p_T - p_{t2}) dp_{t2}. \end{aligned} \quad (10)$$

At the level of current knowledge, leptons have no further structures. However, to produce a lepton in a common process, two participant quarks, a projectile quark and a target quark, are assumed to take part in the interactions. The p_T spectra of leptons are in fact the fold of two TP-like functions, that is Eq. (10) in which m_{01} and m_{02} are empirically the constituent mass of the lightest quark. To produce leptons in a special process such as in $e\bar{e} \rightarrow \mu^+ \mu^-$, m_{01} and m_{02} are the constituent mass of e quark.

There are three participant quarks to constitute usually baryons, namely the quarks 1, 2 and 3. The p_T spectra of baryons are the fold of three TP-like functions. We have the fold of the first two TP-like functions to be

$$\begin{aligned} f_{12}(p_{t12}) &= \int_0^{p_{t12}} f_1(p_{t1}) f_2(p_{t12} - p_{t1}) dp_{t1} \\ &= \int_0^{p_{t12}} f_2(p_{t2}) f_1(p_{t12} - p_{t2}) dp_{t2}. \end{aligned} \quad (11)$$

The fold of the first two TP-like functions and the third

TP-like function is

$$\begin{aligned} f(p_T) &= \int_0^{p_T} f_{12}(p_{t12}) f_3(p_T - p_{t12}) dp_{t12} \\ &= \int_0^{p_T} f_3(p_{t3}) f_{12}(p_T - p_{t3}) dp_{t3}. \end{aligned} \quad (12)$$

Equation (8) can fit approximately the spectra in whole p_T range for various particles at the particle level, in which m_0 is the rest mass of the considered particle. In principle, Eqs. (10) and (12) can fit the spectra in whole p_T range for various particles at the quark level, in which m_{0i} is the constituent mass of the quark i . If Eq. (8) is a revision of Eq. (7), Eqs. (10) and (12) are the results of the multisource model [19, 20] at the quark level. In the multisource model, one, two, or more sources are assumed to emit particles due to different production mechanisms, source temperatures and event samples. In a given event sample, the particles with the same source temperature are assumed to emit from the same source by the same production mechanism. We can also call Eqs. (10) and (12) the results of participant quark model due to they being the contributions of participant quarks.

We would like to explain the normalization constant in detail. As a probability density function, $f(p_T) = (1/N)dN/dp_T$ cannot be used to compare directly with the experimental data presented in literature in some cases, where N denotes the number of considered particles. Generally, the experimental data are presented in forms of i) dN/dp_T , ii) $d^2N/dydp_T$, and iii) $(1/2\pi p_T)d^2N/dydp_T = Ed^3\sigma/dp^3$, where E and p denote the energy and momentum of the considered particle respectively. One can use $N_0 f(p_T)$, $N_0 f(p_T)/dy$, and $(1/2\pi p_T)N_0 f(p_T)/dy$ to fit them accordingly, where N_0 denotes the normalization constant.

Let σ denote the cross-section, the forms of data have usually i) $d\sigma/dp_T$, ii) $d^2\sigma/dydp_T$, and iii) $(1/2\pi p_T)d^2\sigma/dydp_T = Ed^3\sigma/dp^3$. One can use $\sigma_0 f(p_T)$, $\sigma_0 f(p_T)/dy$, and $(1/2\pi p_T)\sigma_0 f(p_T)/dy$ to fit them accordingly, where σ_0 denotes the normalization constant. The data presented in terms of m_T can also be studied due to the conserved probability density and the relation between m_T and p_T . In particular, $(1/2\pi p_T)d^2\sigma/dydp_T = (1/2\pi m_T)d^2\sigma/dydm_T$, where σ can be replaced by N .

III. RESULTS AND DISCUSSION

Figure 1(a) shows the p_T spectra (the invariant cross-section), $Ed^3\sigma/dp^3$, of some hadrons with given combinations and decay channels including $(\pi^+ + \pi^-)/2$ plus $\pi^0 \rightarrow \gamma\gamma$, $(K^+ + K^-)/2$ plus $K_S^0 \rightarrow \pi^0\pi^0$, $\eta \rightarrow \gamma\gamma$ plus $\eta \rightarrow \pi^0\pi^+\pi^-$, $\omega \rightarrow e^+e^-$ plus $\omega \rightarrow \pi^0\pi^+\pi^-$ plus $\omega \rightarrow \pi^0\gamma$, $(p + \bar{p})/2$, $\eta' \rightarrow \eta\pi^+\pi^-$, $\phi \rightarrow e^+e^-$ plus $\phi \rightarrow K^+K^-$, $J/\psi \rightarrow e^+e^-$, and $\psi' \rightarrow e^+e^-$ produced in $p + p$ collisions at 200 GeV. Different symbols represent different particles and their different decay channels measured by the PHENIX Collaboration [14]. The results corresponding to π , K , η , ω , p , and η' are scaled by multiplying 10^6 , 10^5 , 10^4 , 10^3 , 10^2 , and 10 , respectively. The results corresponding to ϕ , J/ψ , and ψ' are not re-scaled.

In Fig. 1(a), the dotted and dashed curves are our fitted results by using Eqs. (8) (for mesons and baryons) and (10) (for mesons) or (12) (for baryons) respectively. The values of free parameters (T , n , and a_0), normalization constant (σ_0), χ^2 , and degree of freedom (dof) obtained from Eq. (8) are listed in Table I, while the values of parameters and χ^2/dof obtained from Eqs. (10) or (12) are listed in Table II. In Eq. (8), m_0 is taken to be orderly the rest mass of π , K , η , ω , p , η' , ϕ , J/ψ , and ψ' for the cases from $(\pi^+ + \pi^-)/2$ to $\psi' \rightarrow e^+e^-$ sequenced due to the order shown in Fig. 1(a). In the fit process at the quark level, the quark structure of π^0 results in its $f(p_T)$ to be the half of the sum of $u\bar{u}$'s $f(p_T)$ and $d\bar{d}$'s $f(p_T)$. Because the constituent masses of u and d are the same [21], π^0 's $f(p_T)$ is equal to $u\bar{u}$'s $f(p_T)$ or $d\bar{d}$'s $f(p_T)$. The quark structure of η results in its $f(p_T)$ to be $\cos^2\phi \times u\bar{u}$'s $f(p_T) + \sin^2\phi \times s\bar{s}$'s $f(p_T)$ due to the quark structures of η_q and η_s , where $\phi = 39.3^\circ \pm 1.0^\circ$ is the mixing angle [22]. The quark structure of η' results in its $f(p_T)$ to be $\sin^2\phi \times u\bar{u}$'s $f(p_T) + \cos^2\phi \times s\bar{s}$'s $f(p_T)$.

To show the departures of the fit from the data, following Fig. 1(a), Figs. 1(b) and 1(c) show the ratios of data to fit obtained from Eqs. (8) and (10) or (12) respectively. One can see that the fits are around the data in whole p_T range, except for a few large departures. The experimental data on the mentioned hadrons measured in $p + p$ collisions at 200 GeV by the PHENIX Collaboration [14] can be fitted by Eqs. (8) (for mesons and baryons) and (10) (for mesons) or (12) (for baryons). From the values of χ^2 and data over fit, one can see that Eq. (10) or (12) seems to be better than Eq. (8).

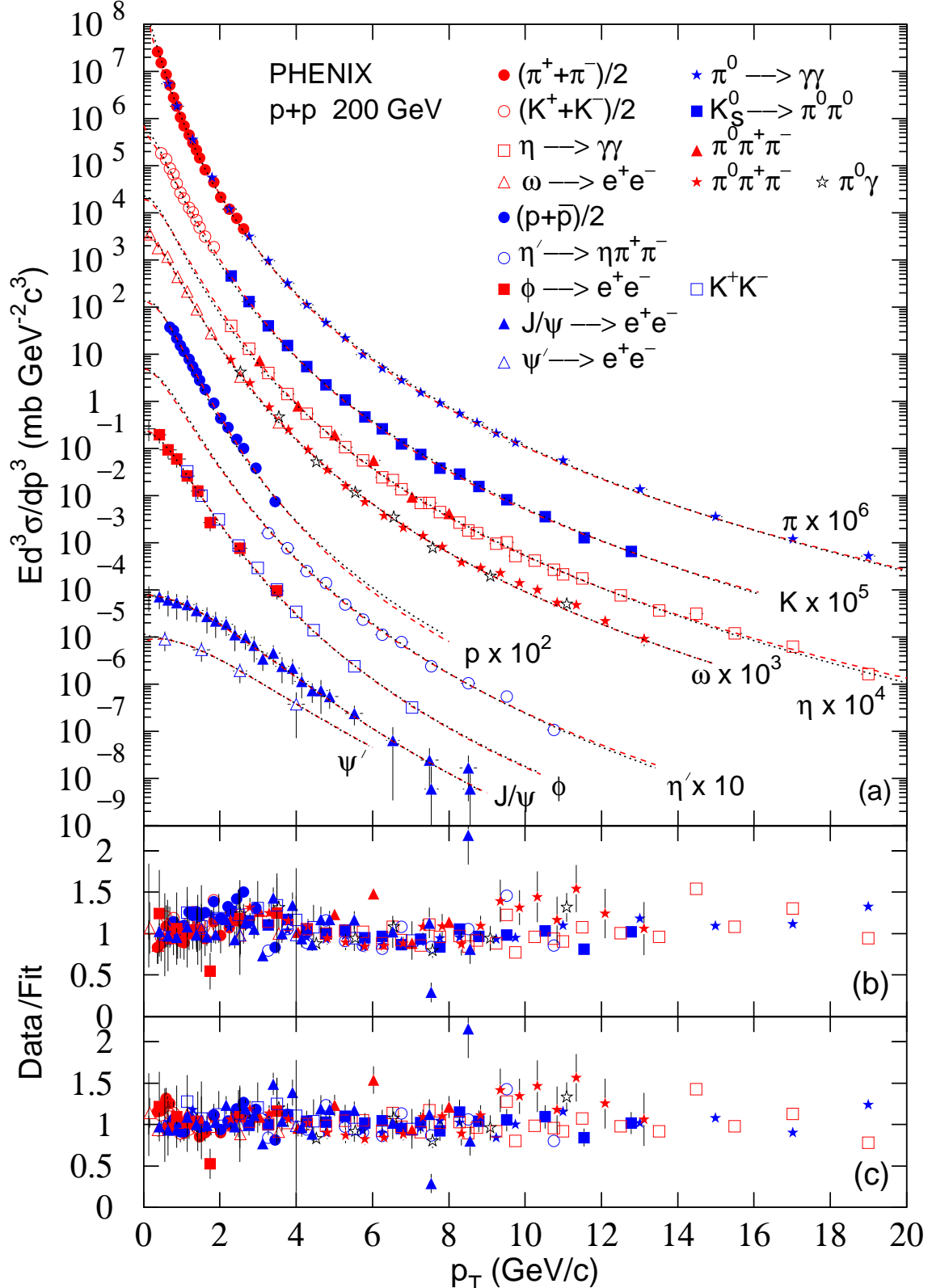


FIG. 1: (a) The invariant cross-section of some hadrons with given combinations and decay channels produced in $p + p$ collisions at 200 GeV. Different symbols represent different particles and their different decay channels measured by the PHENIX Collaboration [14], some of them are scaled by different amounts marked in the panel. The dotted and dashed curves are our fitted results by using Eqs. (8) and (10) or (12) respectively. (b) The ratio of data to fit obtained from Eq. (8). (c) The ratio of data to fit obtained from Eq. (10) or (12).

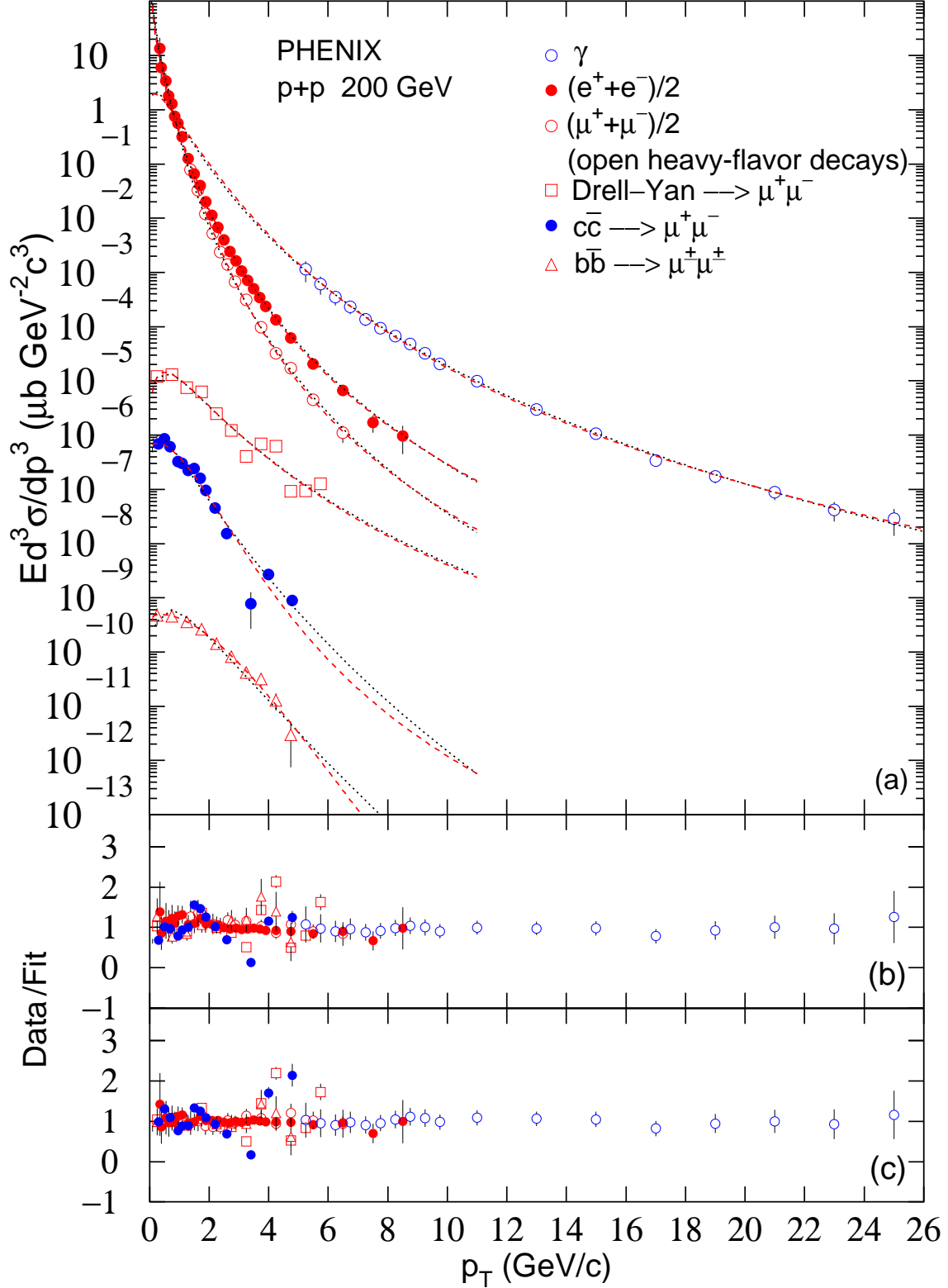


FIG. 2: (a) The invariant cross-section of photons and some leptons with given combinations and producing channels produced in $p+p$ collisions at 200 GeV. Different symbols represent different particles and their producing channels measured by the PHENIX Collaboration [15–18]. The dotted and dashed curves are our fitted results by using Eqs. (8) and (10) respectively. (b) The ratio of data to fit obtained from Eq. (8). (c) The ratio of data to fit obtained from Eq. (10).

TABLE I: Values of T , n , a_0 , σ_0 , χ^2 , and dof corresponding to the dotted curves in Fig. 1, which are fitted by the TP-like function [Eq. (8)]. The last dof is 0 which appears as “–” in the table.

Particle	T (GeV)	n	a_0	σ_0 (mb)	χ^2/dof
$(\pi^+ + \pi^-)/2$	0.128 ± 0.002	9.409 ± 0.200	0.890 ± 0.030	37.042 ± 1.307	5/39
π^0					
$(K^+ + K^-)/2$	0.177 ± 0.002	9.500 ± 0.030	0.887 ± 0.010	3.197 ± 0.044	7/27
K_S^0					
η	0.195 ± 0.002	9.889 ± 0.040	1.000 ± 0.010	1.755 ± 0.088	6/32
ω	0.193 ± 0.001	9.460 ± 0.100	0.900 ± 0.020	3.073 ± 0.065	23/34
$(p + \bar{p})/2$	0.149 ± 0.002	9.100 ± 0.700	1.040 ± 0.030	1.291 ± 0.044	11/13
η'	0.210 ± 0.002	10.001 ± 0.245	0.980 ± 0.002	0.584 ± 0.018	4/8
ϕ	0.204 ± 0.003	9.424 ± 0.185	1.000 ± 0.035	0.307 ± 0.013	11/15
J/ψ	0.416 ± 0.008	11.004 ± 0.450	0.997 ± 0.015	$(5.365 \pm 0.132) \times 10^{-4}$	4/22
ψ'	0.452 ± 0.003	8.349 ± 0.052	0.959 ± 0.010	$(9.234 \pm 0.044) \times 10^{-5}$	1/–

Figure 2(a) shows the invariant cross-section of photons and some leptons with given combinations and producing channels including $(e^+ + e^-)/2$, $(\mu^+ + \mu^-)/2$ (open heavy-flavor decays), Drell–Yan $\rightarrow \mu^+ \mu^-$, $c\bar{c} \rightarrow \mu^+ \mu^-$, and $b\bar{b} \rightarrow \mu^\pm \mu^\pm$ produced in $p + p$ collisions at 200 GeV. Different symbols represent different particles and their producing channels measured by the PHENIX Collaboration [15–18]. The dotted and dashed curves are our fitted results by using Eqs. (8) and (10) respectively, where two participant quarks are considered in the formation of mentioned particles. The values of parameters and χ^2/dof obtained from Eqs. (8) and (10) are listed in Tables III and IV respectively. In Eq. (8), m_0 is taken to be orderly the rest mass of γ , e , μ , 2μ , 2μ , and 4μ for the cases from γ to $b\bar{b} \rightarrow \mu^\pm \mu^\pm$ sequenced due to the order shown in Fig. 2(a). In Eq. (10), $m_{01} + m_{02}$ are taken to be orderly the constituent masses of $u + u$, $u + u$, $u + c$, $u + u$, $c + c$, and $b + b$ sequenced due to the same order as particles.

Following Fig. 2(a), Figs. 2(b) and 2(c) show the ratios of data to fit obtained from Eqs. (8) and (10) respectively. One can see that the fits are around the data in whole p_T range, except for a few large departures. The experimental data on the mentioned photons and leptons measured in $p + p$ collisions at 200 GeV by the PHENIX Collaboration [15–18] can be fitted by Eqs. (8) and (10). From the values of χ^2 and data over fit, one can see that Eq. (10) seems to be better than Eq. (8).

The values of a_0 in Table 1 show that maybe Eq. (8) is not necessary due to $a_0 \approx 1$. However, the values

of a_0 in Table 3 show that Eq. (8) is indeed necessary due to $a_0 \neq 1$. In general, Eq. (8) is necessary in the data-driven analysis due to the fact that $a_0 \neq 1$ in some cases.

To see the dependences of the spectra on free parameters, Figure 3 presents variant pion spectra with different parameters in Eqs. (8) and (10). From the upper panel [Figs. 3(a), 3(b), and 3(c)] to middle panel [Figs. 3(d), 3(e), and 3(f)] then to lower panel [Figs. 3(g), 3(h), and 3(i)], T changes from 0.1 GeV to 0.15 GeV then to 0.2 GeV. From the left panel to middle panel then to right panel, n changes from 5 to 10 then to 15. In each panel, the solid, dotted, dashed, and dot-dashed curves without (with) open circles correspond to the spectra with $a_0 = -0.1, 0, 1$, and 2, respectively, from Eq. (8) [Eq. (10)]. One can see that the probability in high p_T region increases with the increase of T , decreases with the increase of n , and increase with the increase of a_0 . From negative to positive, a_0 determines obviously the shape in low p_T region.

From the shapes of curves in Fig. 3, one can see that the parameter a_0 introduced in the TP-like function [Eq. (8)] by us determines mainly the trend of curve in low- p_T region. If the contribution of resonance decays affect obviously the shape of spectrum in low- p_T region, one may use a more negative a_0 in the fit process. Due to the introduction of a_0 , the TP-like function is more flexible than the Tsallis–Pareto-type function. In fact, a_0 is a sensitive quantity to describe the contribution of resonance decays.

TABLE II: Values of T , n , a_0 , σ_0 , χ^2 , and dof corresponding to the dashed curves in Fig. 1, which are fitted by the fold [Eq. (10) or (12)] of two or three TP-like functions. The last dof is 0 which appears as “–” in the table.

Particle	Quark structure	T (GeV)	n	a_0	σ_0 (mb)	χ^2/dof
$(\pi^+ + \pi^-)/2$	$u\bar{d}, d\bar{u}$	0.205 ± 0.004	7.629 ± 0.025	-0.540 ± 0.020	37.600 ± 4.011	5/39
π^0	$(u\bar{u} - d\bar{d})/\sqrt{2}$					
$(K^+ + K^-)/2$	$u\bar{s}, s\bar{u}$	0.196 ± 0.001	7.816 ± 0.030	-0.091 ± 0.007	2.913 ± 0.044	4/27
K_S^0	$d\bar{s}$					
$\eta: \eta_q, \eta_s$	$(u\bar{u} + d\bar{d})/\sqrt{2}, s\bar{s}$	0.212 ± 0.001	8.109 ± 0.030	0.000 ± 0.011	1.838 ± 0.066	4/32
ω	$(u\bar{u} + d\bar{d})/\sqrt{2}$	0.222 ± 0.001	8.394 ± 0.089	0.000 ± 0.010	2.787 ± 0.124	21/34
$(p + \bar{p})/2$	$uud, \bar{u}\bar{u}\bar{d}$	0.162 ± 0.002	7.600 ± 0.080	-0.130 ± 0.030	1.288 ± 0.029	3/13
$\eta': \eta_q, \eta_s$	$(u\bar{u} + d\bar{d})/\sqrt{2}, s\bar{s}$	0.233 ± 0.002	8.315 ± 0.405	0.000 ± 0.010	0.593 ± 0.022	3/8
ϕ	$s\bar{s}$	0.236 ± 0.003	8.232 ± 0.200	0.000 ± 0.020	0.307 ± 0.018	10/15
J/ψ	$c\bar{c}$	0.439 ± 0.008	8.545 ± 0.035	0.000 ± 0.015	$(5.275 \pm 0.132) \times 10^{-4}$	4/22
ψ'	$c\bar{c}$	0.503 ± 0.005	7.025 ± 0.030	0.055 ± 0.004	$(9.232 \pm 0.044) \times 10^{-5}$	1/–

TABLE III: Values of T , n , a_0 , σ_0 , χ^2 , and dof corresponding to the dotted curves in Fig. 2, which are fitted by the TP-like function [Eq. (8)].

Particle	T (GeV)	n	a_0	σ_0 (μb)	χ^2/dof
γ	0.258 ± 0.001	9.413 ± 0.020	1.750 ± 0.010	4.836 ± 0.044	2/14
$(e^+ + e^-)/2$	0.203 ± 0.002	7.840 ± 0.040	0.002 ± 0.011	14.114 ± 0.371	17/24
$(\mu^+ + \mu^-)/2$	0.125 ± 0.001	9.208 ± 0.050	0.799 ± 0.003	13.486 ± 0.131	5/9
(open heavy-flavor decays)					
Drell-Yan $\rightarrow \mu^+ \mu^-$	0.349 ± 0.003	8.849 ± 0.100	2.200 ± 0.020	$(1.556 \pm 0.125) \times 10^{-4}$	8/8
$c\bar{c} \rightarrow \mu^+ \mu^-$	0.385 ± 0.005	17.200 ± 1.000	1.509 ± 0.008	$(4.197 \pm 0.251) \times 10^{-6}$	10/11
$b\bar{b} \rightarrow \mu^\pm \mu^\pm$	0.489 ± 0.004	30.211 ± 1.000	2.113 ± 0.030	$(7.162 \pm 0.314) \times 10^{-9}$	8/6

IV. SUMMARY AND CONCLUSIONS

We summarize here our main observations and conclusions.

(a) The transverse momentum spectra in terms of the invariant cross-section of various particles (some hadrons with given combinations and decay channels, photons, and some leptons with given combinations and producing channels) produced in high energy proton-proton collisions have been studied by a TP-like function (a revised Tsallis-Pareto-type function). Meanwhile, the transverse momentum spectra have also been studied in the framework of participant quark model or the multisource model at the quark level. In the model, the source itself is exactly the participant quark. Each participant quark contributes the transverse momentum spectrum to be the TP-like function.

(b) For a hadron, the participant quarks are in fact its constituent quarks. The transverse momentum spectrum of the hadron is the fold of two or more TP-like functions. For a lepton, the transverse momentum spectrum is the fold of two TP-like functions due to two participant quarks, e.g. projectile and target quarks, taking part in the collisions. The TP-like function and the fold of a few TP-like functions can fit the experimental data of various particles produced in proton-proton collisions at 200 GeV measured by the PHENIX Collaboration.

(c) In the TP-like function and the fold of a few TP-like functions, the main parameters T , n , and a_0 are sensitive to the spectra. In variant pion spectra from the TP-like function and the fold of two TP-like functions, the probability in high transverse momentum region increases with the increase of T , decreases with the increase of n , and increase with the increase of a_0 . From

TABLE IV: Values of T , n , a_0 , σ_0 , χ^2 , and dof corresponding to the dashed curves in Fig. 2, which are fitted by the fold [Eq. (10)] of two TP-like functions.

Particle	Quark-like	T (GeV)	n	a_0	σ_0 (μb)	χ^2/dof
γ	uu	0.383 ± 0.001	6.793 ± 0.040	0.060 ± 0.002	4.967 ± 0.044	2/14
$(e^+ + e^-)/2$	uu	0.255 ± 0.002	6.378 ± 0.030	-0.696 ± 0.003	13.946 ± 0.176	5/24
$(\mu^+ + \mu^-)/2$	uc	0.167 ± 0.001	5.935 ± 0.055	-0.802 ± 0.003	12.439 ± 0.270	4/9
(open heavy-flavor decays)						
Drell-Yan $\rightarrow \mu^+ \mu^-$	$u\bar{u}$	0.418 ± 0.010	5.616 ± 0.040	0.398 ± 0.008	$(1.560 \pm 0.125) \times 10^{-4}$	8/8
$c\bar{c} \rightarrow \mu^+ \mu^-$	$c\bar{c}$	0.221 ± 0.005	6.402 ± 0.500	0.066 ± 0.010	$(4.051 \pm 0.188) \times 10^{-6}$	7/11
$b\bar{b} \rightarrow \mu^\pm \mu^\pm$	$b\bar{b}$	0.235 ± 0.007	11.253 ± 2.000	0.049 ± 0.020	$(7.162 \pm 0.251) \times 10^{-9}$	3/6

negative to positive, a_0 determines obviously the shape in low transverse momentum region, which is sensitive in describing the contribution of resonance decays.

Acknowledgments

The first author (PPY) thanks Prof. Dr. David Blaschke and his colleagues of Bogoliubov Laboratory for Theoretical Physics of Joint Institute for Nuclear Research (Russia) for their hospitality, in where this work was partly performed. This work was supported by the National Natural Science Foundation of China under Grant Nos. 11575103 and 11847311, the Scientific and Technological Innovation Programs of Higher Education Institutions in Shanxi (STIP) under Grant No. 201802017, the Shanxi Provincial Natural Science Foundation under Grant No. 201701D121005, the Fund for Shanxi “1331 Project” Key Subjects Construction, and the financial supports from ALICE Project No. SR/MF/PS-01/2014-IITI(G) of Department of Science

& Technology, Government of India.

Data Availability

The data used to support the findings of this study are included within the article and are cited at relevant places within the text as references.

Compliance with Ethical Standards

The authors declare that they are in compliance with ethical standards regarding the content of this paper.

Conflicts of Interest

The authors declare that there are no conflicts of interest regarding the publication of this paper. The funders had no role in the design of the study; in the collection, analyses, or interpretation of the data; in the writing of the manuscript, or in the decision to publish the results.

[1] Suleymanov M 2018 *Int. J. Mod. Phys. E* **27** 1850008
[2] Abelev B I *et al* (STAR Collaboration) 2009 *Phys. Rev. C* **79** 034909
[3] Hagedorn R 1983 *Riv. Nuovo Cim.* **6**(10) 1
[4] Tsallis C 1988 *J. Stat. Phys.* **52** 479
[5] Abelev B I *et al* (STAR Collaboration) 2007 *Phys. Rev. C* **75** 064901
[6] Biró T S, Purcsel G and Ürmössy K 2009 *Eur. Phys. J. A* **40** 325
[7] Mizoguchi T, Biyajima M and Suzuki N 2017 *Int. J. Mod. Phys. A* **32** 1750057
[8] Lao H L, Liu F H, Li B C and Duan M Y 2018 *Nucl. Sci. Tech.* **29** 82
[9] Lao H L, Liu F H, Li B C, Duan M Y and Lacey R A 2018 *Nucl. Sci. Tech.* **29** 164
[10] Khachatryan V *et al* (CMS Collaboration) 2010 *J. High Energy Phys.* **2010** 041
[11] Chatrchyan S *et al* (CMS Collaboration) 2012 *Eur. Phys. J. C* **72** 2164
[12] Chatrchyan S *et al* (CMS Collaboration) 2014 *Eur. Phys. J. C* **74** 2847
[13] Sirunyan A M *et al* (CMS Collaboration) 2017 *Phys. Rev. D* **96** 112003
[14] Adare A *et al* (PHENIX Collaboration) 2011 *Phys. Rev.*

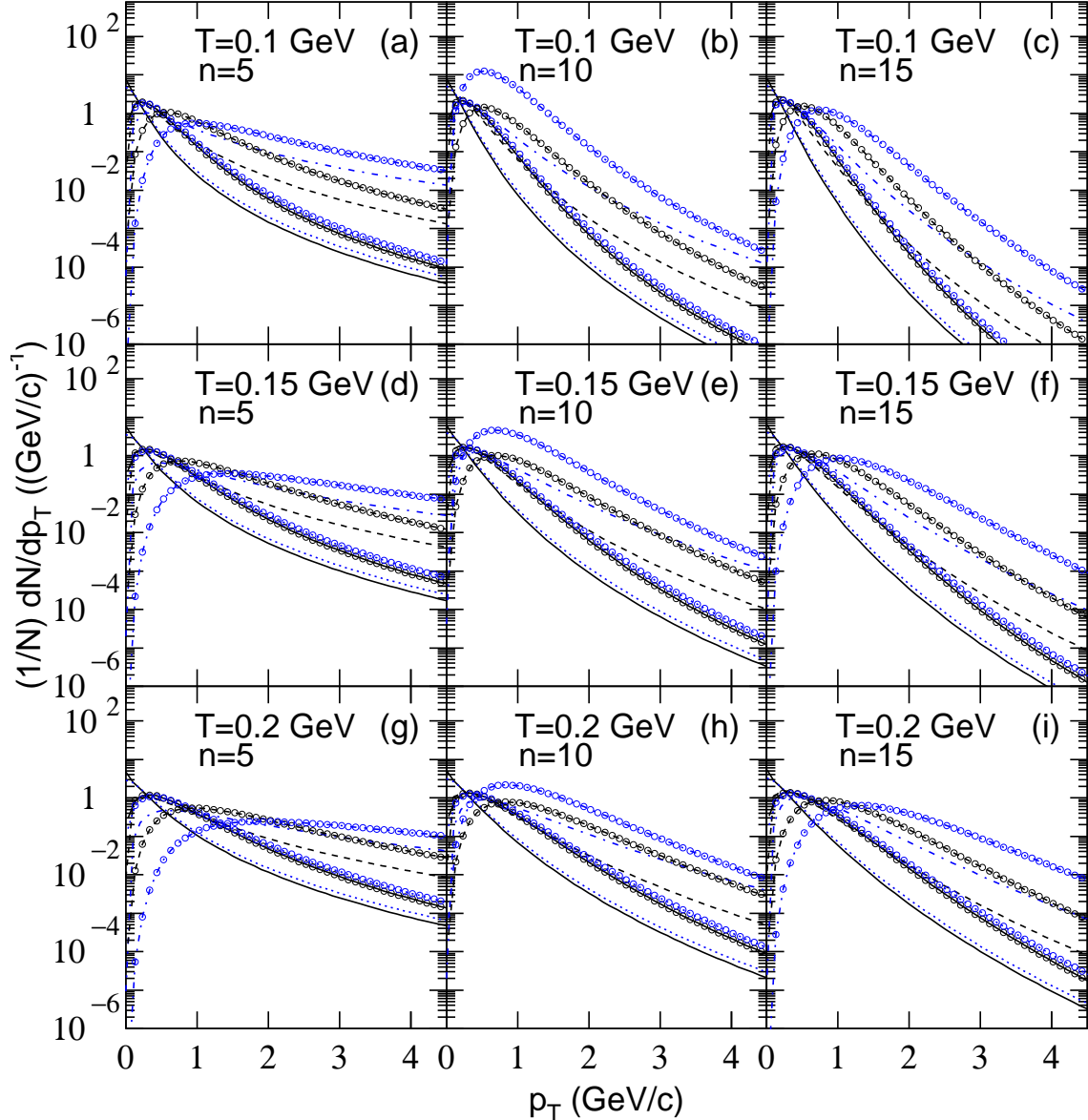


FIG. 3: Variant pion spectra with different parameters in Eqs. (8) and (10). From the upper panel [Figs. 3(a), 3(b), and 3(c)] to middle panel [Figs. 3(d), 3(e), and 3(f)] then to lower panel [Figs. 3(g), 3(h), and 3(i)], T changes from 0.1 GeV to 0.15 GeV then to 0.2 GeV. From the left panel to middle panel then to right panel, n changes from 5 to 10 then to 15. In each panel, the solid, dotted, dashed, and dot-dashed curves without (with) open circles are obtained by $a_0 = -0.1, 0, 1$, and 2, respectively, from Eq. (8) [Eq. (10)].

D **83** 052004

- [15] Adare A *et al* (PHENIX Collaboration) 2011 *Phys. Rev. C* **84** 044905
- [16] Adare A *et al* (PHENIX Collaboration) 2012 *Phys. Rev. D* **86** 072008
- [17] Aidala C *et al* (PHENIX Collaboration) 2019 *Phys. Rev. D* **99** 072003
- [18] Aidala C *et al* (PHENIX Collaboration) 2017 *Phys. Rev.*

D **95** 112001

- [19] Liu F H 2008 *Nucl. Phys. A* **810**, 159
- [20] Liu F H, Gao Y Q, Tian T and Li B C, *Eur. Phys. J. A* **50** 94
- [21] Xiao Z J and Lü C D 2016 *Introduction to Particle Physics*, Science Press, Beijing, China, p. 160
- [22] Feldmann T, Kroll P and Stech B 1998 *Phys. Rev. D* **58** 114006